Replacement of Lys-300 with a glutamine in the NhaA Na^+/H^+ antiporter of *Escherichia coli* yields a functional electrogenic transporter

Received for publication, July 18, 2018, and in revised form, November 6, 2018 Published, Papers in Press, November 8, 2018, DOI 10.1074/jbc.RA118.004903

Miyer Patiño-Ruiz[‡1], **Manish Dwivedi**[§2], **Octavian Călinescu**[‡¶3], **Mehmet Karabel**[‡], **Etana Padan**[§1,4], and **Klaus Fendler**[‡1,5]

From the [‡]*Max-Planck Institute of Biophysics, 60438 Frankfurt am Main, Germany, the* [§]*Institute of Life Sciences, Hebrew University of Jerusalem, 91904 Jerusalem, Israel, and the* [¶]*Department of Biophysics, "Carol Davila" University of Medicine and Pharmacy, 050474 Bucharest, Romania*

Edited by Karen G. Fleming

Much of the research on Na^+/H^+ exchange has been done in prokaryotic models, mainly on the NhaA Na^+/H^+-exchanger from *Escherichia coli* (EcNhaA). Two conserved aspartate residues, Asp-163 and Asp-164, are essential for transport and are candidates for possible binding sites for the two H^+ that are exchanged for one Na^+ to make the overall transport process electrogenic. More recently, a proposed mechanism of transport for EcNhaA has suggested direct binding of one of the transported H^+ to the conserved Lys-300 residue, a salt bridge partner of Asp-163. This contention is supported by a study reporting that substitution of the equivalent residue, Lys-305, of a related Na^+/H^+ antiporter, NapA from *Thermus thermophilus*, renders the transporter electroneutral. In this work, we sought to establish whether the Lys-300 residue and its partner Asp-163 are essential for the electrogenicity of EcNhaA. To that end, we replaced Lys-300 with Gln, either alone or together with the simultaneous substitution of Asp-163 with Asn, and characterized these transporter variants in electrophysiological experiments combined with H^+ transport measurements and stability analysis. We found that K300Q EcNhaA can still support electrogenic Na^+/H^+ antiport in EcNhaA, but has reduced thermal stability. A parallel electrophysiological investigation of the K305Q variant of TtNapA revealed that it is also electrogenic. Furthermore, replacement of both salt bridge partners in the ion-binding site of EcNhaA produced an electrogenic variant (D163N/K300Q). Our findings indicate that alternative mechanisms sustain EcNhaA activity in the absence of canonical ion-binding residues and that the conserved lysines confer structural stability.

Maintaining intracellular pH and sodium content are vital processes for all the living cells. Consequently, organisms have evolved mechanisms that strictly regulate Na^+ and H^+ concentrations across biological membranes. Na^+/H^+ antiporters represent one of these mechanisms.

Na^+/H^+ antiporters of the superfamily of monovalent cation proton antiporters (CPA)[6] are subdivided into two big families, CPA1 and CPA2, and a small family of Na^+-transporting carboxylic acid decarboxylases (1). The prototype CPA1 members are the well-known mammalian NHEs that are mainly responsible for the electroneutral extrusion of protons, in response to intracellular acidification, by using the electrochemical Na^+ gradient generated by the Na^+/K^+-ATPase (2). In contrast, most representative members of the CPA2 family are bacterial Na^+/H^+-exchangers that catalyze the electrogenic exchange of intracellular Na^+ by H^+. EcNhaA (*Escherichia coli* NhaA) is the CPA2 family prototype and has been studied extensively. EcNhaA is indispensable for pH and Na^+ homeostasis in *E. coli* and, in contrast to NHE, utilizes the inwardly-directed electrochemical H^+ gradient generated by the inner membrane H^+-ATPases to export Na^+ (or Li^+) (2) with a stoichiometry $1Na^+$:$2H^+$ (3, 4). Together with the Na^+/H^+-exchanger NhaB, EcNhaA allows *E. coli* to grow under adverse conditions such as high-saline and/or alkaline environments (5). Characteristic for NhaA are its very high turnover (6) and its strongly pH-dependent activity (6), a property it shares with many prokaryotic (7) and eukaryotic Na^+/H^+ antiporters (2, 8–10).

Based on the crystal structure of the electrogenic Na^+/H^+ antiporter EcNhaA and biochemical studies, it has been suggested that the lysine at position 300 plays a central role in the function (11–13) and stability (14) of the antiporter. The latest NhaA crystal structure (15) shows that at acidic pH Lys-300 forms a salt bridge with Asp-163, a residue that is most likely involved in coordinating the transported Na^+ ion together with Asp-164 (Fig. 1) (13, 15–17). Based on this structure, it has been suggested that Na^+ binding to Asp-164 releases the first H^+ of the two exchanged against Na^+. The second proton was pro-

The authors declare that they have no conflicts of interest with the contents of this article.

This article contains Figs. S1–S2.

[1] Supported by DIP (DFG, German-Israeli Project Cooperation Grant LA3655/1-1).

[2] Supported by the PBC, Council for Higher Education, and the Hebrew University Program for Fellowships for Outstanding Postdoctoral Fellows from China and India (2015). Present address: Amity Institute of Biotechnology, Amity University Uttar Pradesh Malhaur, Lucknow-226028, India.

[3] Supported by Ministry of Research and Innovation, CNCS-UEFISCDI, Project No. PN-III-P1-1.1-PD-2016-0802, within PNCDI III.

[4] Supported by Israel Science Foundation Grants 284/12 and 939/14.

[5] To whom correspondence should be addressed: Dept. of Biological Chemistry, Max Planck Institute of Biophysics, Max-von-Laue-Str. 3, 60438 Frankfurt am Main, Germany. Tel.: 49-69-6303-2035; E-mail: fendler@biophys.mpg.de.

[6] The abbreviations used are: CPA, cation proton antiporter; DSF, differential scanning fluorimetry; EcNhaA, NhaA Na^+/H^+-exchanger of *E. coli*; SSM, solid-supported membrane; Bistris propane, 1,3-bis[tris(hydroxymethyl)methylamino]propane; PDB, Protein Data Bank; NHE, Na^+/H^+-exchanger; DDM, *n*-dodecyl-β-D-maltoside; LPR, lipid-to-protein ratio.

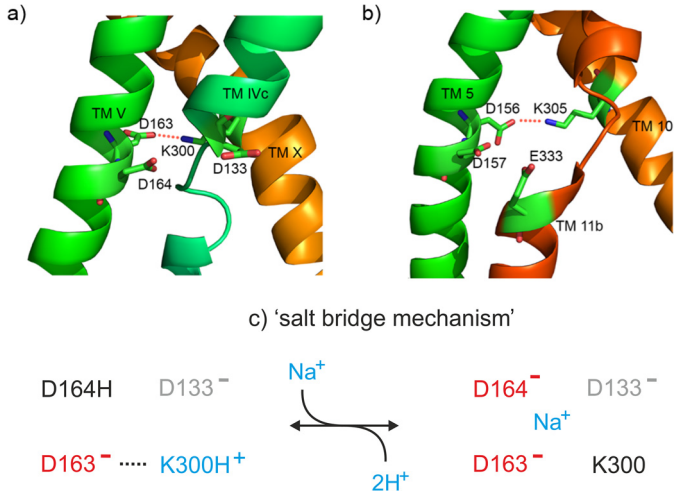

Figure 1. EcNhaA and TtNapA ion-binding pocket. Four charged residues are proposed to contribute to Na^+ and H^+ binding in EcNhaA (PDB code 4AU5 (15)) (*a*) and TtNapA (PDB 5BZ2 (31)) (*b*). *c*, salt bridge mechanism proposed for EcNhaA and TtNapA. Only the relevant residues for EcNhaA are shown. Also aspartate 133 is included, which is proposed to serve as an auxiliary H^+-binding site when the canonical sites Asp-163 and Lys-300 are deleted (see text).

posed to originate from the protonated Lys-300 in the Asp-163/Lys-300 salt bridge in a "salt bridge mechanism" of transport (14). However, replacement of Lys-300 by an arginine (13), which is most likely not able to release its proton (18), or replacement by an uncharged alanine residue showed still appreciable albeit smaller transport currents (14), which is difficult to understand if a strict salt bridge mechanism is in function. In addition, the Lys-300 mutants investigated so far showed significantly reduced structural stability (14), and it is unclear to what extent this instability contributes to the observed reduced functionality of the mutants.

Recent mechanistic and structural analysis of a related electrogenic Na^+/H^+ antiporter, NapA from *Thermus thermophilus* (TtNapA), supports the critical functional role of the homologous lysine residue Lys-305 that forms a salt bridge with one of the Na^+-binding aspartates, Asp-156, and possibly also serves as a proton donor in the salt bridge mechanism. Replacement of Lys-305 by a neutral alanine, polar glutamine, or by a permanently positively charged arginine showed an apparently electroneutral phenotype indicating that only a single H^+ of Asp-157 is exchanged for one Na^+ (19). In addition, the mutation K305Q rescued the nonfunctional D156N mutant implying that an unpaired positive charge in position 305 is lethal for NapA function.

Because the electroneutrality of the TtNapA K305 variants is a central point of the argument in favor of the salt bridge mechanism, we have performed an analysis of the analogous mutations in EcNhaA, namely of K300Q EcNhaA and D163N/K300Q EcNhaA by direct electrophysiological experiments. This was combined with H^+ transport measurements and thermal stability analysis. Finally, to rule out the possibility of a significantly different transport mechanism in TtNapA compared with EcNhaA, we performed a comparative electrophysiological analysis of TtNapA and the corresponding K305Q and D156N/K305Q variants.

Results

Effect of EcNhaA K300Q and D163N/K300Q mutations on the salt resistance of E. coli

To evaluate the growth phenotype of EcNhaA K300Q under conditions of high-salt concentrations, a salt-sensitive strain of *E. coli* (EP432) that lacks the Na^+/H^+ antiporters NhaA and NhaB was employed (20). Only the cells transformed with a functional antiporter able to export Na^+ grow in selective media (0.6 M NaCl at pH 7/pH 8.2 or 0.1 M LiCl at pH 7.0). As expected, the cells transformed with the WT variant grew well under any of the three tested conditions (Fig. 2*a*). Bacteria transformed with the mutant K300Q grew similarly to the WT at pH 7, with a moderate reduction in growth when Na^+ was replaced by Li^+. However, growth was decreased by 3 orders of magnitude under high-Na^+ conditions at pH 8.2 (Fig. 2*a*).

Besides replacement of Lys-300 by Gln, its partner in the salt bridge, Asp-163, was exchanged by Asn. This additional mutation did not further affect the salt-resistance phenotype observed for the single mutant K300Q (Fig. 2*a*).

Fluorescence dequenching assay of EcNhaA in inside-out membrane vesicles

A preliminary characterization of the transport activity mediated by the EcNhaA K300Q and D163N/K300Q mutants was performed using fluorescence-dequenching assays in inside-out (or everted) membrane vesicles isolated from EP432 cells expressing those variants. For comparison, protein expression was quantified in the mutants relative to the WT: 40% in K300Q and 36% for D163N/K300Q EcNhaA. Expression in D163N EcNhaA was 23% (17).

The fluorescent dye acridine orange was used as a probe of the transmembrane H^+ gradient. Energization of the *E. coli* respiratory chain with Tris/D-lactate causing acidification of the vesicles is observed as quenching of the fluorescence (21). If the membrane contains a functional Na^+/H^+-exchanger, addition of Na^+ or Li^+ to the outside of the vesicles triggers $Na^+(Li^+)/H^+$ antiport, which is observed as fluorescence dequenching (22).

Insertion of the single mutation K300Q reduced the Na^+/H^+ antiport activity to ~40% of the WT at pH 8.5 (Fig. 2, *c* and *d*). However, considering that expression of the mutant was only ~1/3 of WT, we have to conclude that in this assay the K300Q EcNhaA variant was as active as the WT. The same effect was observed for the double mutant D163N/K300Q. Once it was established that both variants were active, their substrate affinities were determined. It was found that both mutations remarkably affected the Li^+ K_m (K_m^{Li+}). The K_m values for K300Q (1.1 ± 0.3 mM) and D163N/K300Q (0.5 ± 0.1 mM) (Fig. 2*b*) are 55- and 25-fold higher, respectively, than the value reported for the WT (0.02 mM) (14).

Na^+- and Li^+-induced dequenching appeared to be relatively pH-independent for all the tested variants, except EcNhaA WT at Na^+ 10 mM, which evidenced a reduction of 50% at pH 7.0, while remaining constant over the rest of the tested pH range (7.5–9.0) (Fig. 2, *c* and *d*).

a)

	WT (cells/mL)	K300Q (cells/mL)	D163N-K300Q (cells/mL)	pBR322 (cells/mL)
LBK	3.1×10^8	2.2×10^8	2.0×10^8	2.8×10^8
0.1 M LiCl (pH 7)	2.5×10^8	3.1×10^7	1.4×10^7	-
0.6 M NaCl (pH 7)	2.7×10^8	2.5×10^8	1.4×10^8	-
0.6 M NaCl (pH 8.2)	1.7×10^7	1.5×10^4	1.7×10^4	-

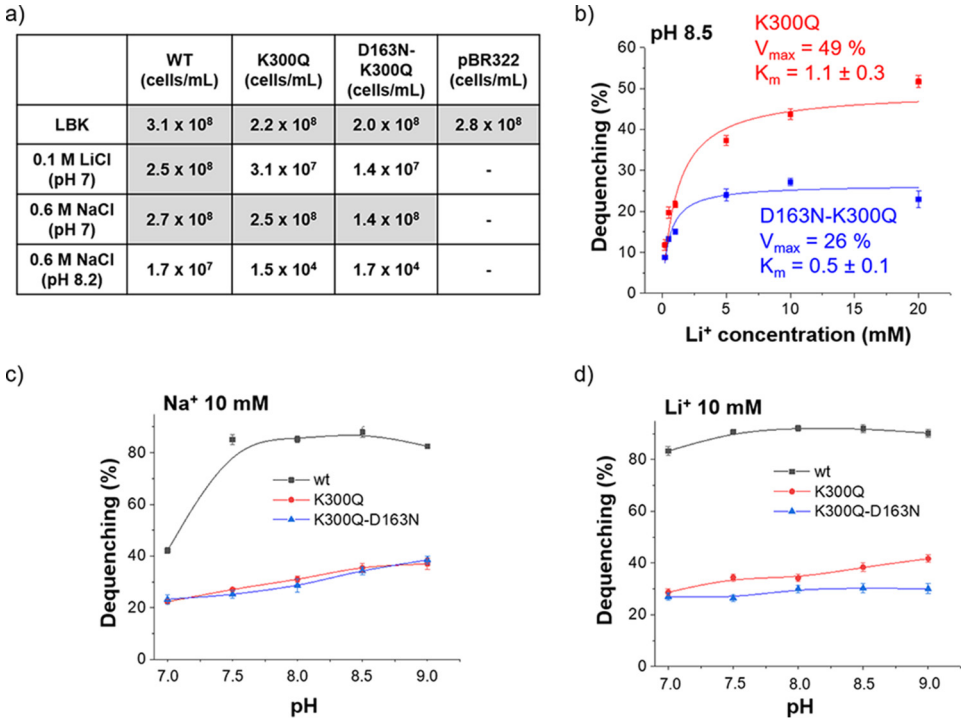

Figure 2. Growth phenotype and Na^+ (Li^+)/H^+ antiport activity of EcNhaA variants in native membranes. *a,* growth phenotype. *Unshaded regions* of the table indicate conditions of poor cell growth (less than 5×10^7 cells/ml). Growth experiments were conducted on agar plates with high Na^+ (0.6 M) or high Li^+ (0.1 M) at the pH values indicated. Growth was calculated as cells/ml after 48 h of incubation at 37 °C as described previously (13). −, no growth. *b–d,* dequenching in inside-out membrane vesicles. Dequenching experiments were performed by energizing the membrane vesicles from the *E. coli* strain EP432 expressing the EcNhaA variants with Tris/D-lactate. Dequenching was obtained upon addition of Na^+ or Li^+. *b,* Li^+ dependence of the dequenching obtained for EcNhaA K300Q (*red*) and D163N/K300Q (*blue*) variants at pH 8.5. Data points were fitted to a hyperbolic equation, and apparent K_m (mM) values were calculated. *c* and *d,* pH dependence of dequenching experiments carried out at Na^+ 10 mM (*c*) and Li^+ 10 mM (*d*), for EcNhaA K300Q (*red*) and D163N/K300Q (*blue*). For comparison WT is included (*black*). Data correspond to the average of three individual experiments and are shown as mean ± S.D.

Functional analysis of EcNhaA variants in proteoliposomes

To characterize the protein transport function, the EcNhaA variants K300Q and D163N/K300Q, were expressed in *E. coli*, detergent-solubilized, purified, and reconstituted in liposomes. Electrogenicity as well as the kinetic parameters for the protein function were determined by SSM electrophysiology (23), whereas the H^+ transport activity was evaluated by dequenching of acridine orange fluorescence in proteoliposomes using pH gradient generated by NH_4^+.

Electrophysiological analysis of EcNhaA K300Q and D163N/K300Q

SSM-based electrophysiological measurements on proteoliposomes of electrogenic CPA2 Na^+/H^+ antiporters are characterized by negative transient currents upon $Na^+(Li^+)$ concentration jumps indicating that a net outward positive charge transfer takes place during the transport cycle (24–26) in agreement with their $1Na^+:2H^+$ stoichiometry (3). In this study, all recorded signals represented steady-state charge transfer according to previously published criteria (14).

Replacing Lys-300 in EcNhaA by a polar Gln residue did not abolish the negative currents obtained for the WT, but showed robust electrogenic transport. However, the single mutation reduced by 40-fold the magnitude of the peak current compared with the values typically observed for the WT variant under the same conditions (Fig. 3, *a* and *b*). An even more drastic reduction was observed for the peak current of the D163N/K300Q variant (120 fold) (Fig. 3*b*). Nevertheless, the persistence of a negative current is a clear indication that even when those two charged residues located in the ion-binding site are replaced by a neutral amino acid the transport activity is still electrogenic. In addition, it was observed that both mutants invariably showed substantial rundown of the electrical signals over a period of 1–2 h, a property that correlates with a tendency to aggregate the solubilized enzymes (13).

A full characterization of the signal obtained for the EcNhaA K300Q mutant with respect to its Na^+ concentration and pH dependence (Table 1 and Fig. 3, *c* and *d*) confirmed that the reduction in current magnitude is not associated with changes in pH profile or Na^+ affinity. The currents of the double mutant D163N/K300Q EcNhaA were too small, and the signals too unstable for a detailed characterization.

Fluorescence dequenching measurements of EcNhaA K300Q and D163N/K300Q

To test the correlation between the electrophysiological results and the H^+ transport activity for both EcNhaA variants, acridine orange fluorescence–dequenching measurements were carried out in proteoliposomes. In contrast to the assay in inside-out membrane vesicles, the H^+ gradient was generated by loading the proteoliposomes with NH_4Cl. Once the proteoliposomes were diluted in NH_4^+-free solution, NH_3 diffuses out, leaving the intra-liposomal compartment acidified. This acidification is observed as a quenching in the fluorescence (Fig. 3*e*). The instability of the established H^+ gradient is evidenced by a subsequent slow increment in the fluorescence.

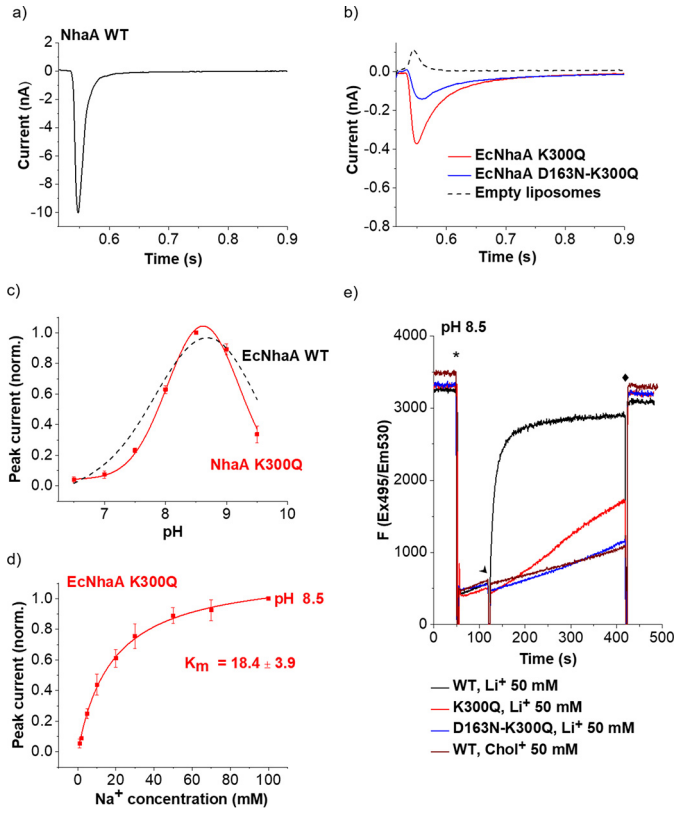

Figure 3. Electrophysiology and H^+ transport activity of EcNhaA variants in proteoliposomes. SSM-based electrophysiological measurements were performed on proteoliposomes or empty liposomes using a single solution exchange protocol as described under "Experimental procedures." Upon a NaCl 100 mM jump at pH 8.5, a transient current representing steady-state charge transfer was obtained for EcNhaA WT (*a*) as well as for the K300Q (*red*) and D163N/K300Q (*blue*) variants tested (*b*). For comparison, the signal obtained for empty liposomes is shown (*dashed line*). *c,* pH dependence of the transient current amplitude recorded after Na^+ 100 mM jumps at pH values between 6.5 and 9.5 for EcNhaA K300Q. Data were normalized to the maximum determined amplitude. For comparison, pH dependence for EcNhaA WT reported in Ref. 24 was included (*dashed line*). *d,* Na^+ dependence of the transient current amplitude recorded for EcNhaA K300Q after Na^+ concentration jumps at pH 8.5. Data were normalized to the maximum data value and K_m (mM) was calculated from the hyperbolic fit. Traces in *a* and *b* correspond to representative results from at least three different recordings. Curves in *c* represent Voigt fits of the experimental data. Data in *c* and *d* are displayed as the average of three different recordings ± S.D. *e,* H^+ transport activity determined by fluorescence dequenching on EcNhaA WT, K300Q, and D163N/K300Q proteoliposomes. Purified and detergent-solubilized variants of EcNhaA were reconstituted in liposomes at LPR 10 and loaded with NH_4Cl to generate a H^+ gradient, acidic inside. Acridine orange was used as a fluorescent probe to detect ΔpH. Fluorescence quenching is obtained when acidified liposomes are added to the medium at pH 8.5, indicated as *. Addition of LiCl to induce dequenching is indicated by an *arrowhead*. As a negative control, choline chloride was added instead of LiCl for the WT. Finally, dissipation of the gradient by addition of $(NH_4)_2SO_4$ 25 mM is marked with ◆. Fluorescence plots correspond to representative data from three different experiments.

If an active Na^+/H^+-exchanger exists in the membrane, dequenching can be induced by addition of Na^+ (or Li^+) to the outside of the liposomes, initiating the $Na^+(Li^+)/H^+$ antiport. As observed in Fig. 3*e*, the WT EcNhaA variant showed robust dequenching (≈90%) following Li^+ addition. In contrast, a remarkably reduced Li^+/H^+ antiport activity was recorded in EcNhaA K300Q proteoliposomes, which agrees with the decreased peak current observed for the same mutant in SSM. In contrast, no dequenching was observed for the D163N/K300Q variant (Fig. 3*e*). This might be an indication of the limitation of this assay on detecting such a small activity corresponding to the dramatically reduced current recorded for the double mutant.

The dequenching assay is difficult to quantify due to inherent problems of the assay like the limited dynamic range (25) and poorly controlled internal pH. But the overall low H^+ transport activity of the K300Q and D163N/K300Q mutants, as determined in the dequenching assay, correlates with a corresponding low electrogenic activity as assessed electrophysiologically.

Thermal stability of EcNhaA K300Q and D163N/K300Q

To establish whether the single and double mutations affected the stability of EcNhaA, two different techniques were employed: differential scanning fluorimetry (DSF) and circular dichroism (CD). Both techniques detect thermal unfolding at rising temperatures of the detergent-solubilized protein. DSF follows the fluorescence emission intensity of the protein's tryptophan and tyrosine residues. If these residues are exposed to a hydrophilic environment as a consequence of temperature-induced structural destabilization, their quantum yield decreases leading to changes in fluorescence wavelength and intensity (28). To account for these changes, the ratio between the emission intensities at 350 and 330 nm ($F_{350/330}$) is plotted against the temperature (Fig. 4*a*). In CD, protein unfolding events can be detected by monitoring ellipticity, which is correlated to the α-helical content of a protein. When a protein unfolds as a result of heating, these highly-ordered secondary structures are lost, which is observed by an intensity change in the CD bands (Fig. 4*b*) (29). The resulting temperature-dependent intensity traces in DSF and CD are known as melting curves.

As reported previously, EcNhaA WT showed a DSF melting curve characterized by a clearly pronounced inflection point at 65.9 °C (Fig. 4*a*) (14). In contrast, the presence of the relatively flat curves obtained for the EcNhaA K300Q and D163N/K300Q variants without a clear melting transition suggests that those mutations impair the structural stability of EcNhaA (Fig. 4*a*) (14). This was confirmed by CD (Fig. 4*c*) in which the protein unfolding occurred at 62.0 ± 0.1 and 63.0 ± 0.1 °C for K300Q and D163N/K300Q, respectively, almost 10 °C lower than the transition temperature T_m obtained for the WT at pH 4 (74.7 ± 0.1 °C) (Fig. 4*c* and Table 1). Thermal stability was also determined for the single mutant D163N using CD spectroscopy. As observed in Fig. 4*c*, this mutation presented a melting curve with an intermediate T_m (67 ± 0.1 °C) indicating that mutation of Lys-300 affects the stability of EcNhaA more profoundly than that of Asp-163.

Analysis of homologous mutations in TtNapA: K305Q and D156N/K305Q

Homologous residues to Lys-300 and Asp-163 in TtNapA are Lys-305 and Asp-156. The functional relevance of their mutation has been presented previously (19). For comparison with our EcNhaA data, we have performed a parallel study of the K305Q and D156N/K305Q TtNapA variants in proteoliposomes using identical assays and conditions. For this purpose, K305Q and D156N/K305Q TtNapA were analyzed in proteoliposomes using SSM-based electrophysiology and fluorescence

Table 1

Comparison of Electrophysiology, H^+ transport activity, and thermal stability results for EcNhaA variants

Maximum peak currents (I_{max}) as well as kinetic parameters K_m^{Na+}, K_m^{Li+}, pH_{opt}^{Na+} were obtained from SSM-based electrophysiology on proteoliposomes upon Na^+ or Li^+ concentration jumps. I_{max} was determined from NaCl 100 mM jumps at pH 8.5. Data shown are the mean of three individual recordings ± S.D. H^+ transport activity was determined from fluorescence dequenching experiments in proteoliposomes using acridine orange as a probe. Results are expressed qualitatively (+++, high dequenching; +, low dequenching; and −, no dequenching). Thermal stability of EcNhaA variants was evaluated using purified and solubilized proteins in DDM 0.03% at pH 4 through DSF and CD. Unfolding transition midpoints or melting temperatures (T_m, °C) were acquired from inflection points in the CD melting curve. Results from DSF were expressed qualitatively as +, when the melting curve showed a well-behaved step function with a clear inflection point, or −, when the shallow progression in the melting curve indicated a less stable variant. ND = not determined.

	EcNhaA WT	EcNhaA K300Q	EcNhaA D163N/K300Q	EcNhaA D163N
I_{max}	12 ± 2 nA	0.30 ± 0.06 nA	0.10 ± 0.04 nA	ND
K_m^{Na+}	11 ± 1 mM (pH 8.5)[a]	18.4 ± 3.9 mM (pH 8.5)	ND	ND
K_m^{Li+}	7.3 mM (pH 8.0)[b]	ND	ND	ND
pH_{opt}^{Na+}	8.8[a]	8.6	ND	ND
Dequenching (liposomes)	+++ (50 mM Li^+)	+ (50 mM Li^+)	− (50 mM Li^+)	ND
Stability (DSF)	+	−	−	ND
T_m (CD)	74.7 ± 0.1 °C	62.0 ± 0.1 °C	63.0 ± 0.1 °C	67.0 ± 0.1 °C

[a] Data were taken from Ref. 24.
[b] Data were taken from Ref. 27.

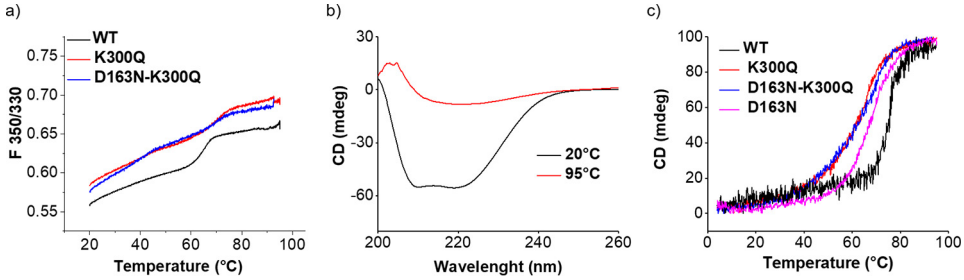

Figure 4. Thermal stability of EcNhaA variants. *a,* melting curves generated by DSF measurements of detergent-solubilized EcNhaA WT, EcNhaA K300Q, and EcNhaA D163N/K300Q at a protein concentration of 0.5 mg/ml and pH 4. The ratio in emission fluorescence intensities at 350 and 330 nm were plotted against the temperature. *b,* comparison of CD spectra generated at 20 and 95 °C for solubilized EcNhaA WT at pH 4. Changes in ellipticity are associated to the loss in secondary structure due to protein unfolding. By following the changes in ellipticity at 221 nm as a function of temperature for EcNhaA WT, K300Q, D163N/K300Q, and D163N, melting curves were obtained. *c,* unfolding transition midpoint (T_m) values were determined from the corresponding inflection points. *Traces* are representative from three different measurements.

dequenching, and thermal stability of the solubilized protein was tested with DSF.

In SSM-based electrophysiology, Na^+ and Li^+ concentration jumps generated negative currents for TtNapA WT and K305Q (Fig. 5, *a* and *b*, and Fig. S1*a*) supporting their electrogenic character and consistent with a transport stoichiometry like that established for EcNhaA WT ($1Na^+$:$2H^+$) (3, 4). The magnitude of the currents recorded for the single mutant K305Q was decreased 12-fold for Na^+ (Fig. 5 and Table 2) and Li^+ (Fig. S1 and Table 2) compared with WT. No currents were detected for the double mutant D156N/K305Q TtNapA. The small positive peak current observed in this case (Fig. 5*b*) has the characteristics of a solution exchange artifact recorded also with empty liposomes (Fig. 3*b*). These results confirm electrogenic transport in WT TtNapA but challenge the notion of electroneutral transport previously proposed for the K305Q variant based on its insensitivity to valinomycin (19).

A complete kinetic analysis of the currents measured on SSM was performed for WT TtNapA as well as for the K305Q variant (Fig. 5, *c* and *d*, and Table 2). A bell-shaped pH dependence (Fig. 5*c*) and increment in K_m^{Na+} values at acidic pH (Table 2) suggest a competition-based transport mechanism of TtNapA similar to that of other CPA2 Na^+/H^+ antiporters (30). Optimal pH and Na^+ affinity are similar to WT EcNhaA (Tables 1 and 2). As in the case of NhaA, the kinetic parameters of TtNapA K305Q did not differ significantly from those obtained for the WT, indicating that the reductions in current magnitude observed for this specific mutation are not due to a change in pH or Na^+ dependence.

As in EcNhaA, the reduction in the current magnitude for the K305Q variant can be correlated with its decreased H^+ transport activity, determined by acridine orange fluorescence dequenching in proteoliposomes. As shown in Fig. 5*e*, addition of 50 mM Li^+ outside the NH_4^+-acidified proteoliposomes generated a rapid and robust fluorescence dequenching for the WT but substantially less dequenching for the K305Q variant and no dequenching at all for the double mutant D156N/K305Q. Compared with the same mutation in EcNhaA, the reduction seemed to be less drastic, which agrees well with the electrophysiological data: 40-fold reduction in EcNhaA K300Q current magnitude compared with only 12-fold for TtNapA K305Q.

As for EcNhaA, the detergent-solubilized protein was tested for thermal unfolding using DSF (Fig. 5*f*). The melting curve of TtNapA WT showed a clear inflection point at high temperature (≈87 °C) as expected for a protein from a thermophile organism. Replacement of Lys-305 by Gln resulted in a flat melting curve with a barely discernible melting transition between 60 and 80 °C, indicating a compromised thermal stability as a consequence of a single point mutation as in K300Q NhaA.

Discussion

NhaA from *E. coli* (EcNhaA) and NapA from *T.thermophilus* (TtNapA) are two related Na^+/H^+-exchangers of the CPA superfamily. They are the only members of the CPA2 family for which structural information is available making them attractive candidates for functional analysis. Both EcNhaA and

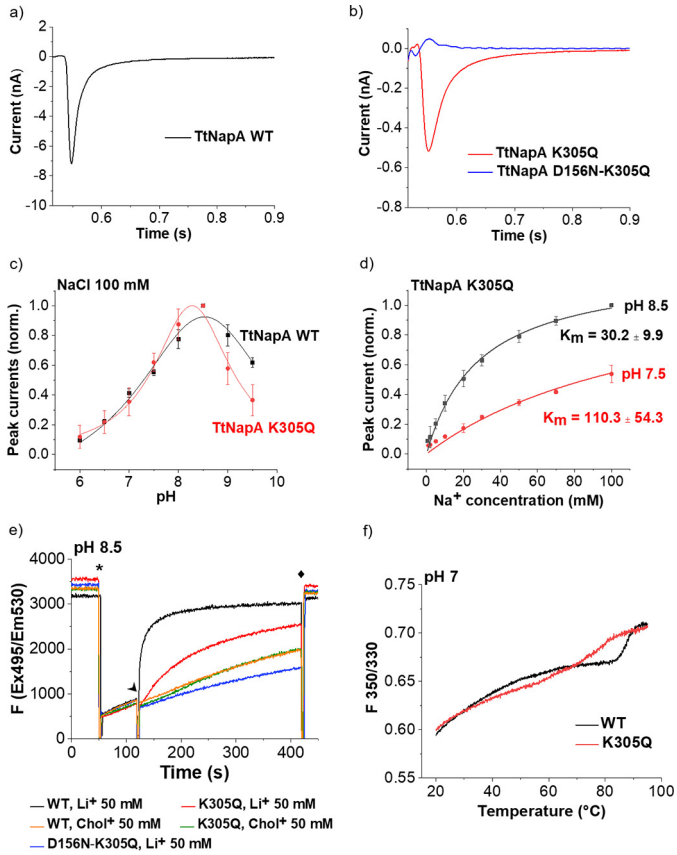

Figure 5. Functional characterization and stability of TtNapA variants. *a* and *b*, current traces obtained by SSM-based electrophysiology upon NaCl 100 mM jumps on LPR 10 proteoliposomes of TtNapA WT (*a*), K305Q (*red*), and D156N/K305Q (*blue*) variants (*b*). *c*, pH dependence of the transient current amplitude recorded after NaCl 100 mM jumps at different pH values for TtNapA WT (*black*) and K305Q variant (*red*). Data from at least three different experiments were normalized to the maximum determined amplitude averaged and presented as mean ± S.D. *Curves* represent Voigt fits of the experimental data. *d*, Na^+ dependence of the transient current amplitude recorded for TtNapA K305Q after Na^+ concentration jumps at pH 8.5 (*black*) and 7.5 (*red*). Data were normalized to the maximum value, averaged and presented as mean ± S.D. K_m (mM) values were calculated from the hyperbolic fits. *e*, H^+ transport activity determined through fluorescence dequenching on TtNapA WT (*black*), K305Q (*red*), and D156N/K305Q (*blue*) proteoliposomes. Purified and detergent-solubilized variants of TtNapA were reconstituted in liposomes at LPR 10 and loaded with NH_4Cl to generate a H^+ gradient, acidic inside. Acridine orange was used as a fluorescent probe to detect ΔpH. Fluorescence quenching is obtained when acidified liposomes are added to the medium at pH 8.5, indicated as *. Addition of LiCl to induce dequenching is indicated by an *arrow*. As a negative control, choline chloride was added instead of LiCl for the WT (*orange*) and K305Q (*green*) variants. Finally, dissipation of the gradient by addition of $(NH_4)_2SO_4$ 25 mM is marked with ♦. Fluorescence plots correspond to representative data from three different experiments. *f*, melting curves generated by DSF measurements of detergent-solubilized TtNapA WT (*black*) and K305Q (*red*) at protein concentrations of 0.5 mg/ml and at pH 7.0 to determine their thermal stability. The ratio in emission fluorescence intensities at 350 and 330 nm were plotted against the temperature.

TtNapA carry lysine residues in immediate proximity of the Na^+-binding site (Lys-300 in EcNhaA and Lys-305 in TtNapA, see Fig. 1), which have been proposed to play a central role in the transport mechanism (11, 13, 14, 17, 19, 31).

As the two transporters, EcNhaA and TtNapA belong to the same family, have highly similar structures and share highly conserved amino acid residues (including Lys-300/Lys-305), it might be expected that the same mutation of a conserved residue would lead to similar effects across the two transporters. Therefore, to reconcile the roles proposed for Lys-300 in EcNhaA and Lys-305 in TtNapA, we investigated the function and stability of the EcNhaA K300Q and D163N/K300Q variants, compared with that of the WT, and assessed whether the consequences of these mutations are the same as they were when mutating the corresponding residues in TtNapA.

Replacement of Lys-300 in EcNhaA by a glutamine impairs its structural stability

Both thermofluorescence as well as the temperature dependence of the CD spectrum (Fig. 4) clearly show a decreased resistance of the K300Q and the D163N/K300Q mutants of EcNhaA to thermal unfolding. This seems to be a general property of Lys-300 variants, and the phenomenon was suggested to rely on the absence of the stabilizing the Lys-300/Asp-163 salt bridge (14). Indeed, mutating also the 2nd partner of the salt bridge, like in the double mutant D163N/K300Q, did not change its thermal stability compared with the single K300Q mutation. Furthermore, the single D163N mutation also showed a decreased melting temperature (Table 1 and Fig. 4). The fact that a stable protein requires that both charged residues, Lys-300 and Asp-163, are in place suggests that the salt bridge is the relevant stability-conferring element rather than the positive charge of Lys-300 as put forward previously (11).

Although the observed melting temperatures are consistently above 60 °C, denaturation of Lys-300 mutants starts as low as 35 °C (Fig. 4*c*), and a tendency for aggregation (in the detergent-solubilized enzyme) and signal rundown (in the SSM experiments) is obvious even at room temperature (13). In consequence, it cannot be ruled out that all or a part of the activity reduction caused by the K300Q and D163N/K300Q mutations is a secondary effect caused by a partially unfolded enzyme. This has to be taken into account for the correct interpretation of the reduced transport activities of the mutants.

Replacement of Lys-300 in EcNhaA by a glutamine yields an active transporter capable of Na^+/H^+ and Li^+/H^+ exchange

Although Lys-300 is obviously essential for the Na^+/H^+-exchanger activity of EcNhaA, a number of replacements of this residue can still perform functional exchange. The mutations that were shown to be tolerated best were replacements of Lys-300 with other amino acids having positively charged side chains like arginine and histidine (13, 14). However, even the uncharged residues cysteine and alanine supported a residual transport function (12, 14). Here, we show that replacement of Lys-300 with glutamine has a robust Na^+/H^+ and Li^+/H^+ exchange activity (Fig. 2). In fact, taking into account the somewhat lower expression of the variants (40% K300Q and 36% D163N/K300Q compared with WT), the K300Q mutant displays a transport activity close to WT in the assays based on native membranes shown in Fig. 2, although the dequenching assay in proteoliposomes shows a more differentiated picture (Fig. 3*e*).

K300Q mutation rescues activity in inactive D163N EcNhaA

The double mutant D163N/K300Q confers salt resistance and displays Na^+/H^+ exchange activity in the membrane-dequenching assays (Fig. 2) demonstrating rescue of the inactive

Table 2

Comparison of electrophysiological activity and thermal stability of TtNapA variants

Maximum peak currents (I_{max}) as well as kinetic parameters K_m^{Na+}, K_m^{Li+}, pH_{opt}^{Na+}, and pH_{opt}^{Li+} were obtained from SSM-based electrophysiology on proteoliposomes using Na^+ or Li^+ concentration jumps. I_{max} was determined from NaCl 100 mM jumps at pH 8.5. Data represent the mean of three individual recordings ± S.D. H^+ transport activity was determined from fluorescence dequenching experiments in proteoliposomes using acridine orange as a probe. Results are expressed qualitatively (+++, high dequenching; +, low dequenching; and −, no dequenching). Thermal stability of TtNapA WT and K305Q variants was evaluated using purified and solubilized proteins in DDM 0.03% at pH 7 by DSF. Results are expressed qualitatively as +, when the melting curve showed a well-behaved step function with a clear inflection point, or −, when a shallow progression in the melting curve or inflection points at lower temperatures indicated a less stable variant. ND = not determined.

	TtNapA WT	TtNapA K305Q	TtNapA D156N/K305Q
I_{max}	5.2 ± 2.0 nA	0.43 ± 0.07 nA	0 nA
K_m^{Na+}	18 ± 3 mM (pH 8.5) 219 ± 9 mM (pH 6.5)	30 ± 10 mM (pH 8.5)	ND
K_m^{Li+}	4.3 ± 2.5 (pH 8.5) 45 ± 17 mM (pH 6.5)	2.9 ± 1.4 mM (pH 8.5)	ND
pH_{opt}^{Na+}	8.5	8.3	ND
pH_{opt}^{Li+}	8.4	8.0	ND
Dequenching (liposomes)	+++ (50 mM Li^+)	+ (50 mM Li^+)	− (50 mM Li^+)
Stability (DSF)	+	−	ND

single mutant D163N EcNhaA (17). A similar phenotype has been observed in the TtNapA Na^+/H^+-exchanger (19), where the corresponding D156N/K305Q double variant was shown to have a significant activity. As discussed above, stability is not restored in the double mutant D163N/K300Q (Fig. 4) ruling out the possibility that the rescuing effect is due to an increased structural stability of the double mutant. The double mutant is of particular interest because in D163N/K300Q EcNhaA two potential H^+ donors/acceptors are deleted in the Na^+/H^+-exchanger binding site while still maintaining transport function.

K300Q EcNhaA is electrogenic

In the electrophysiological SSM experiments, a Na^+ (or Li^+) gradient is applied to the proteoliposomes (Fig. 3). In WT EcNhaA, a negative current is generated under these conditions implying that net positive charge is transported out of the proteoliposomes (Fig. 3*a*). This has been interpreted as a $2H^+/1Na^+$ exchange process (24), as determined previously for EcNhaA (3). Also in K300Q EcNhaA, the transport process is obviously electrogenic, and a negative current is observed implying a H^+/Na^+ stoichiometry of >1.

Stoichiometry is an important determinant for the transport mechanism. In view of the small currents observed in K300Q EcNhaA, we have in parallel assessed its H^+ transport capacity using a dequenching assay in the same proteoliposomes. Although the liposomal dequenching assays are difficult to quantify, it seems clear that H^+ transport in the K300Q mutant is much lower than WT as is the case for the transporter currents. Hence, there is no obvious discrepancy between H^+ transport and charge displacement in proteoliposomes, which is consistent with the assumption that the $2H^+/1Na^+$ stoichiometry is maintained in the mutant. However, a reduced electrogenicity of the K300Q variant represented by a stoichiometry ratio H^+/Na^+ <2 (but >1) cannot be ruled out.

Quantitative differences in the activity of K300Q variants determined in native membranes or proteoliposomes

A comparison of K300Q EcNhaA Na^+/H^+-exchanger activity points to a discrepancy between antiporter activity in proteoliposomes, cells, and native isolated inverted membrane vesicles. The H^+ transport activity of K300Q EcNhaA in membrane vesicles is lower, if at all, by about 2-fold, as compared with the WT (Fig. 2), whereas in proteoliposomes Li^+/H^+-exchange of the variant is much slower (Fig. 3*d*), and transport currents are ~40 times lower than WT (Fig. 3, *a* and *b*). It therefore seems that H^+ transport (dequenching) and currents, both measured in proteoliposomes, are compatible, although the assays involving native membranes, salt resistance, and dequenching in membrane vesicles show a much higher activity of the mutant compared with WT. A similar argument applies to the D163N/K300Q double variant.

What is the reason for the apparently different transport activity of the mutant protein in proteoliposomes and membranes or membrane vesicles? The discrepancy may indicate that the activity of the purified and reconstituted mutant exchangers is reduced compared with that in native membranes, due to the reduced structural stability of the Lys-300 variants in detergent micelles (Fig. 4) (14). Alternatively, the difference in assay protocols may add to the quantitative difference, which needs more experiments to confirm, one explanation being the previously shown limited dynamic range of the fluorescence-dequenching assay in membrane vesicles (25).

EcNhaA is still active and electrogenic when two putative H^+ donors are deleted

Replacement of one of the two aspartates in positions 163 and 164 by nonprotonable side chains has been shown to be lethal for transport function in EcNhaA (13), as is the case also for D156N TtNapA (19). However, in TtNapA, the double mutation K305Q/D156N rescued activity and showed transport albeit with an electroneutral phenotype (19). Our data partly confirm the results obtained in TtNapA, namely that the K300Q replacement (K305Q in TtNapA) rescues activity in the inactive D163N variant (D156N in TtNapA), but in contrast to TtNapA (Fig. 5*b*) (19) the resulting double mutant in EcNhaA D163N/K300Q is clearly electrogenic (Fig. 3*b*).

What are the implications of these results? Based on structural and functional analysis, it was concluded that the binding site of EcNhaA consists only of three potential H^+-binding sites (Asp-163, Asp-164, and Lys-300 (13)), two of which are deleted in the D163N/K300Q mutant (see Fig. 5). However, the observed negative current requires that more than one H^+ is transported for one Na^+. An additional acidic residue, which could contribute to H^+ translocation, is Asp-133 (13, 32). Therefore, we suggest that the mechanism of Na^+/H^+-exchangers may contain a certain amount of redundancy (14)

allowing the exchanger to switch to a different mechanism if an essential structural part is not available. To this effect, the two H^+ may bind to Asp-164 and Asp-133 in the D163N/K300Q EcNhaA variant (Fig. 1) providing electrogenic Na^+/H^+ exchange with a H^+/Na^+ stoichiometry of >1.

Electrophysiological phenotypes of TtNapA WT and its K305Q variants

To obtain a more general picture of the effect of the Lys-300 mutation on the Na^+/H^+-exchanger function, a comparison with a related Na^+/H^+-exchanger is of interest. The transport activity of the *T. thermophilus* Na^+/H^+-exchanger NapA and many of its variants is well characterized using biochemical assays (19, 33, 34), although an electrophysiological characterization was still lacking. Indeed, the electrophysiological comparison of the two companion WT exchangers shows a remarkably consistent picture (Figs. 3 and 5). Both rely on a competition-based transport mechanism (30) with comparable kinetic parameters (Table 2). This makes TtNapA a well suited system for the assessment of the impact of the Lys-300 mutation in EcNhaA.

An analysis of the corresponding K305Q and D156N/K305Q variants of TtNapA shows overall a similar picture as in EcNhaA but also subtle differences. Like its K300Q EcNhaA counterpart, the K305Q variant of TtNapA has a reduced thermal stability (Fig. 5*f*), is clearly electrogenic (Fig. 5, *a* and *d*), and its currents are significantly reduced compared with WT. Therefore, as for K300Q EcNhaA, we have to conclude that transport in K305Q TtNapA proceeds with a H^+/Na^+ stoichiometry of >1.

In contrast to EcNhaA, rescue of the D156N-inactive TtNapA variant by the K305Q mutation was not observed (Table 2 and Fig. 5). This could be a consequence of insufficient sensitivity because in EcNhaA the signals of the D163N/K300Q variant were close to the detection limit of the electrophysiological assay. In fact, based on a somewhat different assay protocol, activity has been previously detected for D156N/K305Q TtNapA (19).

Electrogenicity of K305Q TtNapA is in disagreement with the previous qualification of TtNapA K305Q as electroneutral based on its valinomycin insensitivity (19). However, valinomycin insensitivity is not always a reliable criterion for electroneutral transport especially when the involved charge displacements are small (10× smaller currents than WT, see Table 2) and/or the rate-limiting step is electroneutral (35). In comparison, a current measurement is direct proof for the electrogenicity, which can hardly be disregarded.

Mechanistic implications

Interpretation of data from Lys-300 EcNhaA mutants is complicated by the fact that Lys-300 is not only mechanistically important but also relevant for the structural stability of the protein (Fig. 4) (14). Therefore, it is not always clear whether the reduced activity of a particular Lys-300 variant is a consequence of an impaired transport mechanism or of a partially unfolded protein. A similar conclusion can now be drawn for the Lys-305 mutants of TtNapA (Fig. 5). An additional problem is given by the different H^+ transport assays performed in cells, membrane vesicles, or proteoliposomes using active H^+ transport systems like ATPases and the respiratory chain or NH_4^+ gradients to generate the driving protonmotive force. These assays, although qualitatively in agreement, yield significantly different transport activities. Under these circumstances quantitative determination of, for instance, transport stoichiometry is difficult.

Nevertheless, electrophysiological data with the K300Q EcNhaA and the K305Q TtNapA variants show that the lysine residue is not indispensable for electrogenicity and that also in its absence, and hence in the absence of the salt bridge, more than 1 H^+ is exchanged for 1 Na^+. This rules out the Asp-163/Lys-300 (Asp-156/Lys-305 for TtNapA) salt bridge as an exclusive H^+-binding site. More precisely, the data are compatible with a $2H^+/1Na^+$ exchange stoichiometry of the variants. However, a reduced electrogenicity resulting from a partially uncoupled mechanism with a stoichiometry ranging between 1 and 2 cannot be ruled out. In such a partially uncoupled mechanism, H^+ translocation takes place with either 1 or 2 H^+ in parallel. We have previously suggested that in the WT the function of the Asp-163/Lys-300 salt bridge may be to prevent transport with only 1 H^+ (14). It is therefore conceivable that in the K300Q (K305Q for TtNapA) variant, where salt bridge formation is not possible, an intermediate stoichiometry between 1 and 2 is obtained by allowing transport with 1 or 2 H^+ alternatively.

The presence of an isolated positive charge, Lys-300^+ (Lys-305^+), as is the case in the D163N (D156N) variant, completely abrogates transport, whereas neutralization of both partners of the Asp-163/Lys-300 (Asp-156/Lys-305) salt bridge in the double mutant restores function (this study and Ref. 19). Obviously the presence of an uncompensated positive charge in the binding site is detrimental for substrate binding and transport as suggested previously for TtNapA and now confirmed for EcNhaA (19). This is an alternative argument why the Asp-163/Lys-300 (Asp-156/Lys-305) salt bridge is essential for proper function of the Na^+/H^+ antiporters.

Interestingly, D163N/K300Q EcNhaA is still electrogenic, although two putative H^+-binding sites are missing. Electrogenicity requires at least two H^+-binding sites, and we suggest that Asp-133 plays the role of an auxiliary H^+-binding site in case one of the canonical H^+-binding sites Asp-163 or Asp-164 are not available (13, 32). In the amino acid sequence of TtNapA, there is no conserved Asp residue equivalent to Asp-133 of EcNhaA, although, in the crystal structure, the side chain of Glu-333 in TtNapA occupies a similar position to that of the Asp-133 chain of EcNhaA (Fig. 1) (34). It is possible, however, that Glu-333 of TtNapA cannot serve as an auxiliary H^+-binding site, which would explain why D156N/K305Q TtNapA is electroneutral, whereas D163N/K300Q EcNhaA is electrogenic.

Overall, our findings, along with those of a previous study investigating a number of Lys-300 mutants in EcNhaA (14), show that the conserved lysines in the binding sites of EcNhaA and also TtNapA confer structural stability to the exchangers. Furthermore, electrogenicity of transport does not depend on the presence of Lys-300 (in EcNhaA) or Lys-305 (in TtNapA), which implies that a recently postulated (salt bridge) mechanism for H^+ translocation in EcNhaA (15) and TtNapA (19) is

either incorrect or only one of several different possible mechanisms. Such mechanistic redundancy is also supported by the detection of electrogenic transport in an EcNhaA variant (D163N/K300Q) where two putative H^+-binding sites are deleted. It is not unlikely that these principles also apply to other Na^+/H^+-exchangers of the CPA2 family.

Experimental procedures

Genetic constructs

Variants of EcNhaA in which Lys-300 was replaced were obtained in plasmid pAXH3, a pET20b derivative (36). PCR-based, site-directed mutagenesis was used with pAXH3 as a template. The DNA of each construct was sequenced to verify the mutation.

Salt resistance assays

Survival of *E. coli* EP432 (20) expressing EcNhaA variants K300Q and D163N/K300Q under conditions of high concentrations of Na^+ or Li^+ at pH 7 or 8.2 was assessed as described previously (13).

Determination of Na^+, Li^+/H^+ antiporter activity in isolated inside-out membrane vesicles and apparent K_m determination

Inside-out membrane vesicles from EP432 transformed with the respective plasmids were prepared as described previously (37). Inside-out membrane vesicles were used to determine Na^+/H^+ or Li^+/H^+ antiporter activity with an assay based on the measurement of Na^+- or Li^+-induced changes in the ΔpH as measured by acridine orange, a fluorescent probe of ΔpH (21). The fluorescence assay was performed in a 2.5-ml reaction mixture containing 100–150 μg of membrane protein, 0.1 μM acridine orange, 150 mM choline chloride, 50 mM Bistris propane, and 5 mM $MgCl_2$, and pH was titrated with HCl. Membrane vesicles were energized by addition of 2 mM Tris/D-lactate, inducing proton pumping into the vesicles and fluorescence quenching of the acridine orange dye. Dequenching of fluorescence upon addition of either Na^+ or Li^+ indicates that protons are exiting the vesicles in antiport with either cation. As shown previously (22), the end level of dequenching can be used as an estimate of antiporter activity, and the ion concentration that gives half-maximal dequenching can estimate the apparent K_m value of the antiporter activity. For determination of the apparent K_m values, the end level of dequenching for different concentrations of the tested cations (0.2–20 mM) at the indicated pH levels was used, and the apparent K_m values were calculated by linear regression of a Lineweaver-Burk plot.

Overexpression, purification, and reconstitution

EcNhaA K300Q and D163N/K300Q variants were overexpressed as C-terminally His-tagged proteins in *E. coli* BL21 (DE3) cells and purified in *n*-dodecyl-β-D-maltoside (DDM) detergent using immobilized metal-affinity chromatography as described previously (38). TtNapA WT, K305Q, and D156N/K305Q proteins were produced and purified as described in Ref. 19 and kindly provided by Dr. David Drew's lab (Department of Biochemistry and Biophysics, Stockholm University). Reconstitution of the purified proteins into proteoliposomes was performed using *E. coli* polar lipid extract (Avanti Polar Lipids, Alabaster, AL) at a lipid-to-protein ratio (LPR) of 10, essentially as described previously (24). Reconstitution was tested by SDS-PAGE and Western blotting (Fig. S2).

Detection of Na^+, Li^+/H^+ antiporter activity in proteoliposomes

Proteoliposomes containing any of the EcNhaA or TtNapA variants were loaded with NH_4Cl to generate a H^+ gradient across the membrane. 100 μl of LPR 10 proteoliposomes at a lipid concentration of 10 mg/ml were collected by ultracentrifugation at 100,000 × *g* during 30 min at 4 °C, washed, and resuspended in 30 μl of loading buffer containing MES 10 mM, K_2SO_4 2.5 mM, $MgSO_4$ 5 mM, $(NH_4)_2SO_4$ 100 mM titrated to pH 7 with Tris. The exchange of intra-liposomal conditions was achieved by three freeze-thawing cycles and a final step of a 30-s sonication. 5 μl of the loaded proteoliposomes were diluted in 1 ml of reaction buffer containing MES 10 mM, pH 8.5, sucrose 300 mM, K_2SO_4 2.5 mM, $MgSO_4$ 5 mM, and acridine orange 2 μM. To detect electrogenic transport activity, valinomycin was added to a final concentration of 0.2 μM.

Acridine orange senses the ΔpH (acidic in the proteoliposomes) that was observed by quenching of the fluorescence. Then, the Li^+/H^+ exchange activity was induced by addition of Li^+ 50 mM (as Li_2SO_4) and was observed as dequenching of the fluorescence if an active transporter is present in the proteoliposomes. As a control, choline chloride was added instead of LiCl to a final concentration of 50 mM. Finally, the pH gradient was dissipated by addition of $(NH_4)_2SO_4$ to a final concentration of 25 mM. Empty liposomes were also tested as a control. Fluorescence was followed at an emission wavelength of 530 nm upon excitation at 495 nm using a Hitachi F4500 spectrofluorometer (Hitachi High-Technologies Corp., Tokyo, Japan).

SSM-based electrophysiology

Electrophysiological measurements were performed as described previously (24). Briefly, an octadecanethiol/phospholipid hybrid bilayer was formed on an SSM sensor by adding 2 μl of a mixture of diphytanoyl-*sn*-glycerophosphatidylcholine and octadecylamine (60:1) in decane. On top of the preformed bilayer, 30 μl of proteoliposomes at LPR 10 were added and allowed to absorb for at least 1 h. Empty liposomes were used as a control.

A rapid single-solution exchange protocol (23) was employed on the SSM sensor in the order nonactivating – activating – nonactivating. All solutions contained 25 mM MES, 25 mM MOPS, 25 mM Tris, 100 mM KCl, 5 mM $MgCl_2$, and 1 mM DTT and were titrated to the desired pH with HCl or KOH. In addition, nonactivating solutions contained 200 mM extra KCl, whereas activating solutions contained *x* mM NaCl (or LiCl) and (200 − *x*) mM KCl instead. The amplitude of the recorded transient currents was used as a measure of steady-state transport activity.

Differential scanning fluorometry

Protein stability of the purified EcNhaA and TtNapA variants was analyzed essentially as described previously (14). In brief, glass capillaries were loaded with ~10 μl of protein at a concentration of 0.5 mg/ml in buffer containing KCl 100 mM, $MgCl_2$ 5 mM, DDM 0.03%, potassium acetate 25 mM (pH 4) or

KCl 100 mM, $MgCl_2$ 5 mM, 25 mM Tris 25 mM, HEPES 25 mM (pH 7.0) and placed in the thermal plate of a Prometheus NT.48 instrument (NanoTemper Technologies, Munich, Germany). Temperature was increased in a range from 20 to 95 °C at a heating rate of 1 °C/min. Thermal protein unfolding was followed by monitoring the tryptophan fluorescence at emission wavelengths of 350 and 330 nm upon excitation at 280 nm with an excitation power setting of 10%.

Melting curves were obtained by plotting the ratio of the two emission intensities ($F_{350/330}$) *versus* the temperature. The thermal unfolding transition midpoint or melting temperature (T_m, °C) corresponded to the inflection point of the melting curves and was estimated via first derivative analysis.

Circular dichroism

CD measurements were made on a JASCO J-810 CD spectropolarimeter (JASCO, Inc., Japan), using the supplied Spectra Manager software. The respective proteins (3–4 μM) were prepared in a solution containing 100 mM choline chloride, 5 mM $MgCl_2$, 25 mM citric acid, 10% sucrose, and 0.015% DDM. The corresponding pH values were obtained by titration with KOH or HCl. Spectral data were collected at 0.1-nm intervals at 4 °C, using a Peltier-controlled sample compartment, and variable temperature measurements were made between 4 and 95 °C at a wavelength of observed higher peak (near 221 nm) with 0.2 °C data interval. T_m was determined by plotting data in a sigmoidal curve.

Author contributions—M. P.-R., M. D., O. C., M. K., and K. F. data curation; M. P.-R., M. D., O. C., M. K., and K. F. formal analysis; M. P.-R., M. D., O. C., E. P., and K. F. investigation; M. P.-R., M. D., O. C., E. P., and K. F. writing-original draft; M. P.-R., M. D., O. C., E. P., and K. F. writing-review and editing; E. P. and K. F. conceptualization; E. P. and K. F. supervision; E. P. and K. F. funding acquisition; E. P. and K. F. project administration.

Acknowledgments—We thank Oliver Stehling and colleagues from the University of Marburg Core Facilities Protein Biochemistry and Protein Spectroscopy for help with the DSF measurements as well as David Drew from the Stockholm University, Department of Biochemistry and Biophysics for providing protein of the TtNapA variants.

References

1. Brett, C. L., Donowitz, M., and Rao, R. (2005) Evolutionary origins of eukaryotic sodium/proton exchangers. *Am. J. Physiol. Cell Physiol.* **288,** C223–C239 CrossRef Medline
2. Orlowski, J., and Grinstein, S. (2004) Diversity of the mammalian sodium/proton exchanger SLC9 gene family. *Pflugers Arch.* **447,** 549–565 CrossRef Medline
3. Taglicht, D., Padan, E., and Schuldiner, S. (1993) Proton-sodium stoichiometry of NhaA, an electrogenic antiporter from *Escherichia coli*. *J. Biol. Chem.* **268,** 5382–5387 Medline
4. Dwivedi, M., Sukenik, S., Friedler, A., and Padan, E. (2016) The Ec-NhaA antiporter switches from antagonistic to synergistic antiport upon a single point mutation. *Sci. Rep.* 6, 23339 CrossRef Medline
5. Padan, E., Venturi, M., Gerchman, Y., and Dover, N. (2001) Na^+/H^+ antiporters. *Biochim. Biophys. Acta* **1505,** 144–157 CrossRef Medline
6. Taglicht, D., Padan, E., and Schuldiner, S. (1991) Overproduction and purification of a functional Na^+/H^+ antiporter coded by nhaA (ant) from *Escherichia coli*. *J. Biol. Chem.* **266,** 11289–11294 Medline
7. Padan, E., Bibi, E., Ito, M., and Krulwich, T. A. (2005) Alkaline pH homeostasis in bacteria: new insights. *Biochim. Biophys. Acta* **1717,** 67–88 CrossRef Medline
8. Orlowski, J., and Grinstein, S. (2007) Emerging roles of alkali cation/proton exchangers in organellar homeostasis. *Curr. Opin. Cell Biol.* **19,** 483–492 CrossRef Medline
9. Putney, L. K., Denker, S. P., and Barber, D. L. (2002) The changing face of the Na^+/H^+ exchanger, NHE1: structure, regulation, and cellular actions. *Annu. Rev. Pharmacol. Toxicol.* **42,** 527–552 CrossRef Medline
10. Wakabayashi, S., Hisamitsu, T., Pang, T., and Shigekawa, M. (2003) Mutations of Arg440 and Gly455/Gly456 oppositely change pH sensing of Na^+/H^+ exchanger 1. *J. Biol. Chem.* **278,** 11828–11835 CrossRef Medline
11. Hunte, C., Screpanti, E., Venturi, M., Rimon, A., Padan, E., and Michel, H. (2005) Structure of a Na^+/H^+ antiporter and insights into mechanism of action and regulation by pH. *Nature* **435,** 1197–1202 CrossRef Medline
12. Kozachkov, L., Herz, K., and Padan, E. (2007) Functional and structural interactions of the transmembrane domain X of NhaA, Na^+/H^+ antiporter of *Escherichia coli*, at physiological pH. *Biochemistry* **46,** 2419–2430 CrossRef Medline
13. Maes, M., Rimon, A., Kozachkov-Magrisso, L., Friedler, A., and Padan, E. (2012) Revealing the ligand binding site of NhaA Na^+ /H^+ antiporter and its pH dependence. *J. Biol. Chem.* **287,** 38150–38157 CrossRef Medline
14. Călinescu, O., Dwivedi, M., Patiño-Ruiz, M., Padan, E., and Fendler, K. (2017) Lysine 300 is essential for stability but not for electrogenic transport of the *Escherichia coli* NhaA Na^+/H^+ antiporter. *J. Biol. Chem.* **292,** 7932–7941 CrossRef Medline
15. Lee, C., Yashiro, S., Dotson, D. L., Uzdavinys, P., Iwata, S., Sansom, M. S., von Ballmoos, C., Beckstein, O., Drew, D., and Cameron, A. D. (2014) Crystal structure of the sodium–proton antiporter NhaA dimer and new mechanistic insights. *J. Gen. Physiol.* **144,** 529–544 CrossRef Medline
16. Inoue, H., Noumi, T., Tsuchiya, T., and Kanazawa, H. (1995) Essential aspartic acid residues, Asp-133, Asp-163 and Asp-164, in the transmembrane helices of a Na^+/H^+ antiporter (NhaA) from *Escherichia coli*. *FEBS Lett.* **363,** 264–268 CrossRef Medline
17. Olkhova, E., Kozachkov, L., Padan, E., and Michel, H. (2009) Combined computational and biochemical study reveals the importance of electrostatic interactions between the "pH sensor" and the cation binding site of the sodium/proton antiporter NhaA of *Escherichia coli*. *Proteins* **76,** 548–559 CrossRef Medline
18. Harms, M. J., Schlessman, J. L., Sue, G. R., and García-Moreno, E. B. (2011) Arginine residues at internal positions in a protein are always charged. *Proc. Natl. Acad. Sci. U.S.A.* **108,** 18954–18959 CrossRef Medline
19. Uzdavinys, P., Coinçon, M., Nji, E., Ndi, M., Winkelmann, I., von Ballmoos, C., and Drew, D. (2017) Dissecting the proton transport pathway in electrogenic Na^+/H^+ antiporters. *Proc. Natl. Acad. Sci. U.S.A.* **114,** E1101–E1110 CrossRef Medline
20. Pinner, E., Kotler, Y., Padan, E., and Schuldiner, S. (1993) Physiological role of NhaB, a specific Na^+/H^+ antiporter in *Escherichia coli*. *J. Biol. Chem.* **268,** 1729–1734 Medline
21. Rosen, B. P. (1986) Ion extrusion systems in *Escherichia coli*. *Methods Enzymol.* **125,** 328–336 CrossRef Medline
22. Schuldiner, S., and Fishkes, H. (1978) Sodium-proton antiport in isolated membrane vesicles of *Escherichia coli*. *Biochemistry* **17,** 706–711 CrossRef Medline
23. Schulz, P., Garcia-Celma, J. J., and Fendler, K. (2008) SSM-based electrophysiology. *Methods* **46,** 97–103 CrossRef Medline
24. Mager, T., Rimon, A., Padan, E., and Fendler, K. (2011) Transport mechanism and pH regulation of the Na^+/H^+ antiporter NhaA from *Escherichia coli*: an electrophysiological study. *J. Biol. Chem.* **286,** 23570–23581 CrossRef Medline
25. Călinescu, O., Danner, E., Böhm, M., Hunte, C., and Fendler, K. (2014) Species differences in bacterial NhaA Na^+/H^+ exchangers. *FEBS Lett.* **588,** 3111–3116 CrossRef Medline
26. Lentes, C. J., Mir, S. H., Boehm, M., Ganea, C., Fendler, K., and Hunte, C. (2014) Molecular characterization of the Na^+/H^+-antiporter NhaA from *Salmonella typhimurium*. *PLoS ONE* **9,** e101575 CrossRef Medline
27. Zuber, D., Krause, R., Venturi, M., Padan, E., Bamberg, E., and Fendler, K. (2005) Kinetics of charge translocation in the passive downhill uptake

mode of the Na^+/H^+ antiporter NhaA of *Escherichia coli*. *Biochim. Biophys. Acta* **1709,** 240–250 CrossRef Medline
28. Weichel, M., Bassarab, S., and Garidel, P. (2008) Probing thermal stability of mAbs by intrinsic tryptophan fluorescence. *Bioprocess Int.* **6,** 42–52
29. Greenfield, N. J. (2006) Using circular dichroism collected as a function of temperature to determine the thermodynamics of protein unfolding and binding interactions. *Nat. Protoc.* **1,** 2527–2535 CrossRef Medline
30. Călinescu, O., and Fendler, K. (2015) A universal mechanism for transport and regulation of CPA sodium proton exchangers. *Biol. Chem.* **396,** 1091–1096 Medline
31. Coincon, M., Uzdavinys, P., Nji, E., Dotson, D. L., Winkelmann, I., Abdul-Hussein, S., Cameron, A. D., Beckstein, O., and Drew, D. (2016) Crystal structures reveal the molecular basis of ion translocation in sodium/proton antiporters. *Nat. Struct. Mol. Biol.* **23,** 248–255 CrossRef Medline
32. Rimon, A., Dwivedi, M., Friedler, A., and Padan, E. (2018) Asp133 Residue in NhaA Na^+/H^+ antiporter is required for stability cation binding and transport. *J. Mol. Biol.* **430,** 867–880 CrossRef Medline
33. Furrer, E. M., Ronchetti, M. F., Verrey, F., and Pos, K. M. (2007) Functional characterization of a NapA Na^+/H^+ antiporter from *Thermus thermophilus*. *FEBS Lett.* **581,** 572–578 CrossRef Medline
34. Lee, C., Kang, H. J., von Ballmoos, C., Newstead, S., Uzdavinys, P., Dotson, D. L., Iwata, S., Beckstein, O., Cameron, A. D., and Drew, D. (2013) A two-domain elevator mechanism for sodium/proton antiport. *Nature* **501,** 573–577 CrossRef Medline
35. Alkoby, D., Rimon, A., Budak, M., Patino-Ruiz, M., Călinescu, O., Fendler, K., and Padan, E. (2014) NhaA Na^+/H^+ antiporter mutants that hardly react to the membrane potential. *PLoS ONE* **9,** e93200 CrossRef Medline
36. Rimon, A., Tzubery, T., and Padan, E. (2007) Monomers of the NhaA Na^+/H^+ antiporter of *Escherichia coli* are fully functional yet dimers are beneficial under extreme stress conditions at alkaline pH in the presence of Na^+ or Li^+. *J. Biol. Chem.* **282,** 26810–26821 CrossRef Medline
37. Goldberg, E. B., Arbel, T., Chen, J., Karpel, R., Mackie, G. A., Schuldiner, S., and Padan, E. (1987) Characterization of a Na^+/H^+ antiporter gene of *Escherichia coli*. *Proc. Natl. Acad. Sci. U.S.A.* **84,** 2615–2619 CrossRef Medline
38. Venturi, M., and Padan, E. (2003) in *Membrane Protein Purification and Crystallization: A Practical Guide* (Hunte, C., von Jagow, G., and Schägger, H., eds) pp. 179–190, Elsevier Science, New York